„Babeş - Bolyai" University Cluj - Napoca
Faculty of Chemistry and Chemical Engineering
Doctoral School of Chemical Engineering

HYDROGEN PEROXIDE ELECTROSYNTHESIS USING CATHODES FROM COMMERCIAL AND RECYCLED CARBONACEOUS MATERIALS

PhD THESIS ABRSTACT

Scientific supervisor
Prof. Dr. Eng. Petru ILEA

PhD Student
Eng. Ana-Domnica MĂRINCEAN (căs. Rus)

Cluj-Napoca
2019

„Babeş - Bolyai" University Cluj - Napoca
Faculty of Chemistry and Chemical Engineering
Doctoral School of Chemical Engineering

Eng. Ana-Domnica MĂRINCEAN (căs. Rus)

HYDROGEN PEROXIDE ELECTROSYNTHESIS USING CATHODES FROM COMMERCIAL AND RECYCLED CARBONACEOUS MATERIALS

PhD THESIS ABSTRACT

Jury

President:

Prof. Dr. Eng. CĂLIN-CRISTIAN CORMOȘ, „Babeş - Bolyai" University, Cluj - Napoca

Scientific supervisor

Prof. Dr. Eng. PETRU ILEA, „Babeş - Bolyai" University, Cluj - Napoca

Reviewers

Prof. Dr. Eng. DĂNUT-IONEL VĂIREANU, Politehnica University, Bucharest

Prof. Dr. Eng. NICOLAE VASZILCSIN, Politehnica University Timisoara

Prof. Dr. Eng. GRAZIELLA LIANA TURDEAN, „Babeş - Bolyai" University, Cluj - Napoca

Defense 28.11.2019

TABLE OF CONTENT

Keywords: *hydrogen peroxide electrosynthesis, filter press reactor, carbonaceous materials, 3D electrodes, recycled graphite granules*

Abbreviations and symbols

Abbreviations

A.T.	anolyte tank
A.W.M.	air-water mixer
C.E.	counter electrode
C.E.M.	cation exchanges membrane
C.T.	catholyte tank
D.E.	detector electrode
EAOPs	electrochemical advances oxidation processes
EF	electro-Fenton
FPER	filter press electrochemical reactor
FTHPD	flow-through hydrogen peroxide detector
GB	graphite bloc
GF	graphite felt
RGG	recycled graphite granules
GPP	global parameters of performance
HPE	hydrogen peroxide electrosynthesis
HVL	hydrodynamic linear voltammetry
IPP	intermediate parameters of performance
ISEA	*in situ* electroactivation
Px	pump number x
rrO	reduction reaction of oxygen
RVC	reticulate vitreous carbon
Ref.	reference electrode
W.E.	working electrode

Symbols

C.Ef.	current efficiency, %;
$C.Ef._G$	global current efficiency, %;
$E_{W.E.}$	working electrode potential, [V];
$E_{W.E.max,\ min}$	maximum or minimum applied potential at working electrode, [V];
$I_{D.E.}$	current intensity recorded with detector electrode, [A];
$I_{W.E.}$	current intensity recorded with working electrode, [A];
Q_{air}	air flow, [mL/min];
Q_{el}	electrolyte flow, [mL/min];
t	duration of experiment or step, [s];
t_f	final time, [s];
Δt	duration segments, [s];
W_S	energy specific consumption, [kWh/kg];
$W_{S.G}$	global energy specific consumption, [kWh/kg];
$[H_2O_2]$	hydrogen peroxide concentration, [mg/L];
$[H_2O_2]_f$	final hydrogen peroxide concentration, [mg/L].

INTRODUCTION

In the last decade, the problems related to water pollution are increasing constantly and are mainly caused by the increase of population number and industrialization, urban development, unsustainable use of natural resources and due to the use of inefficient wastewater treatment methods. This situation has led to the elaboration of environment protection legislation and to the issuance of directives with demand for development of effective methods for pollutants elimination from wastewater [1].

In this context, many new treatment processes methods have been developed. Among these methods the most studied are the electrochemical advanced oxidation processes (EAOPs) due to their advantages. EAOPs are based on the generation of a strong oxidant, most often on the generation of the $HO^{\bullet}$ radical [2].

Among the EAOPs, electro-Fenton (EF) processes are the most commonly used for wastewater treatment. The EF process involves the continuous generation of H_2O_2 by the reduction reaction of O_2 (rrO) and obtaining the $HO^{\bullet}$ radical by the Fe^{2+} ions catalyzed decomposition of H_2O_2. The efficiency of the treatment processes are strongly influenced by hydrogen peroxide electrosynthesis (HPE) [3, 4].

Part I: LITERATURE OVERVIEW

Hydrogen peroxide (H_2O_2) is one of the most widely used chemicals in the world. It presents applications in different industries, such as paper production, textile production and metallurgy. It is also used for the synthesis of chemicals and recently, it can be noted an increase in interest for the use of H_2O_2 in processes of treatment and/or purification of water as a source of $HO^{\bullet}$ radical [5, 6]. In this context, H_2O_2 synthesis is a major step in the wastewater treatment, so, many studies are carried out to improve the existing methods or to develop new methods for H_2O_2 production [7-15].

As the method of H_2O_2 obtaining, HPE through rrO is intensely studied, but there are many issues still not elucidated and new opportunities to increase the efficiency of HPE based on the application of advanced electrochemistry engineering and materials science (electrocatalysts) [16-19].

The HPE process is strongly influenced by a number of parameters such as: the nature of the cathode material, the amount of dissolved O_2 in the electrolyte solution, the

applied current density, the pH and composition of the electrolyte solution, the configuration of the electrochemical reactor and the working temperature.

The cathode material has the greatest influence on the HPE process. In this context, in order to increase the efficiency of the HPE process, many materials were tested as cathode for HPE. Among these materials, the most intensively studied are the 3D carbon materials due to their advantages [20-29].

Because of the low O_2 solubility in aqueous solutions at ambient temperature, different ways to provide the O_2 requirement are also studied. The way of introducing O_2 into the process has a major impact on the related costs of HPE process [30].

Also, in order to choose the electrolyte and its pH value, it is generally necessary to take into account the subsequent use of the generated H_2O_2. If H_2O_2 is desired in the paper industry, HPE is used in an alkaline medium. If H_2O_2 is used in EF process, especially in homogeneous EF, HPE in acidic medium will be chosen [31] and depending on the nature of the electrolyte solution, besides $HO^{\bullet}$, other oxidizing agents can be obtained which leads to an efficiency increase of the purification process, but, in this case, toxic by-compounds can be obtained too [8].

Both divided and undivided electrochemical reactors were used for HPE. Undivided electrochemical reactors have the advantage that HPE can be made at lower costs due to lower energy loss but, in this case, H_2O_2 can react on the anode surface. On the contrary, in the divided reactors, by the existence of the interpolar separator, the oxidation of H_2O_2 is prevented but energy is lost. Among the reactors available for HPE, the filter press electrochemical reactor (FPER) is intensively studied due to the advantages related to the flow of electrolyte inside of it [32-38].

Several possibilities have been tested for increase the efficiency or for HPE process intensification. Most often cathode surface modification by physical or chemical methods, mass transport intensification and the possibility of achievement a main cathodic process with secondary anodic process or of a main anodic process with secondary cathodic processes were studied [39-53].

Part II: PESONAL CONTRIBUTIONS

The main objective of this work was to carry out the EAO process with the lowest costs (using air as a source of O_2, a dilute solution of Na_2SO_4 as an electrolyte background and commercial carbonaceous materials untreated/unmodified or recycled) and with the highest efficiency to make the EAO process convenient at industrial level and applicable for water treatment processes.

3. Investigation techniques

In the present thesis, electrochemical methods were used for HPE study and chemical and electrochemical methods were used for monitoring the HPE process by determination of H_2O_2 concentration [54].

For HPE study, hydrodynamic linear voltammetry (HLV) measurements and preparative electrosynthesis studies in potentiostatic and galvanostatic mode were made.

To monitor the HPE process by determining the concentration of electrosynthesized H_2O_2, volumetric, spectrometric and amperometric methods were tested. Among this methods, were selected permanganometric and amperometric method. For the amperometric determination of H_2O_2 an original flow-through hydrogen peroxide detector (FTHPD) was developed and calibrated [55, 56]. The HPE process was continuously monitored by FTHPD and the H_2O_2 concentration at the end of the HPE tests was evaluated by correlating the currents recorded by FTHPD with the H_2O_2 concentration obtained by titration with $KMnO_4$.

4. HPE study

For the HPE study, an experimental setup, described schematically in Fig. 4.1, was developed. This setup included as main constituent: a modified Micro Flow®Cell FPER, FTHPD, tanks for anolyte (A.T.) and catholyte (C.T.) solutions, peristaltic pumps for transport of electrolyte (P1 și P2) and air (P4), a pneumatic pump for electrolyte aeration (P3) during HVL measurements, a centrifugal pump used as air-water mixer (A.W.M.) and

the systems for electrode potential measurement (Ref.1-3). Depending on the measurements, the experimental setup can be composed of the anodic circuit (A) and the cathodic circuit (B) or (C).

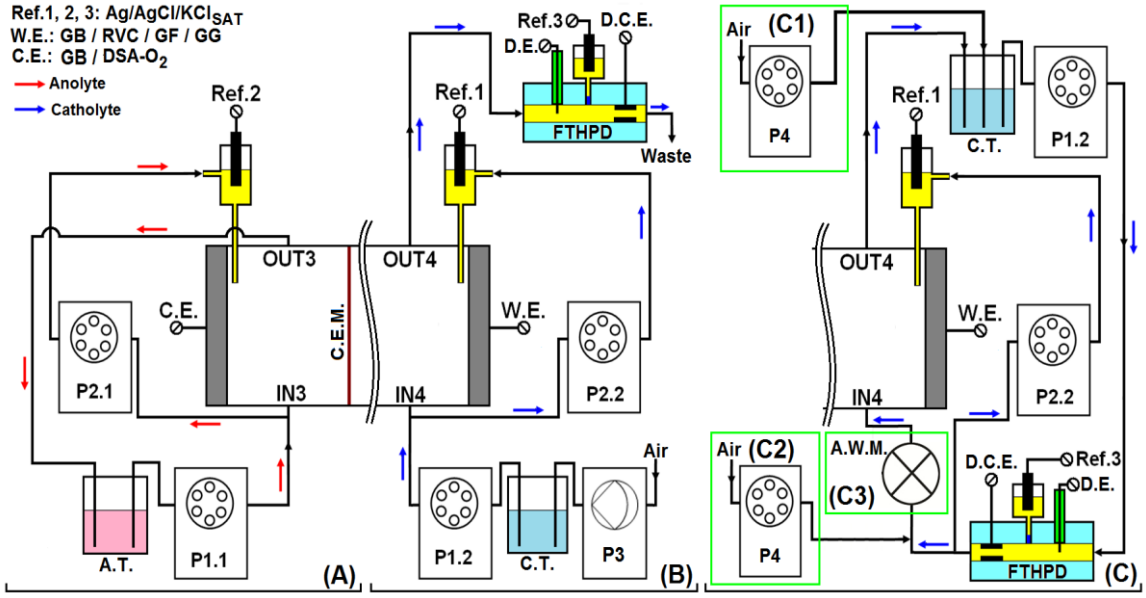

Figure 4.1. Experimental setup for HPE study

The FPER was equipped with Nafion 117 cation exchanges membrane (C.E.M.) and Luggin capillaries, made of PTFE tubes, were introduced into each compartment for electrodes potential measurement. The FPER was equipped with working electrode (W.E.) manufactured from graphite bloc (GB), reticulate vitreous carbon (RVC) with porosity of 100 and 500 ppi, graphite felt (GF) and recycled graphite granules (RGG). As counter electrode (C.E.) was used DSA-O_2 for all HPE tests and GB was used for electro activation tests. The active surface of the materials tested for HPE was 10 cm^2.

FTHPD was positioned at the outlet of the FPER when HLV measurements were performed and at the inlet of the reactor where HPE tests were made. To achieve the most accurate monitoring of HPE using FTHPD, before each HPE test, the detector electrode (D.E.) was conditioned by applying a preset protocol.

For all measurements, as electrolytic support, an aqueous solution of 0.05 M Na_2SO_4 with pH $\approx$ 4.2 was used. The solutions were introduced in the reactor compartments using P1.1-2 pumps and in the reference electrode compartments with P2.1-2.

Depending on the chosen cathode material, different configurations of the cathode compartment of the FPER were assembled (Fig 4.2.)

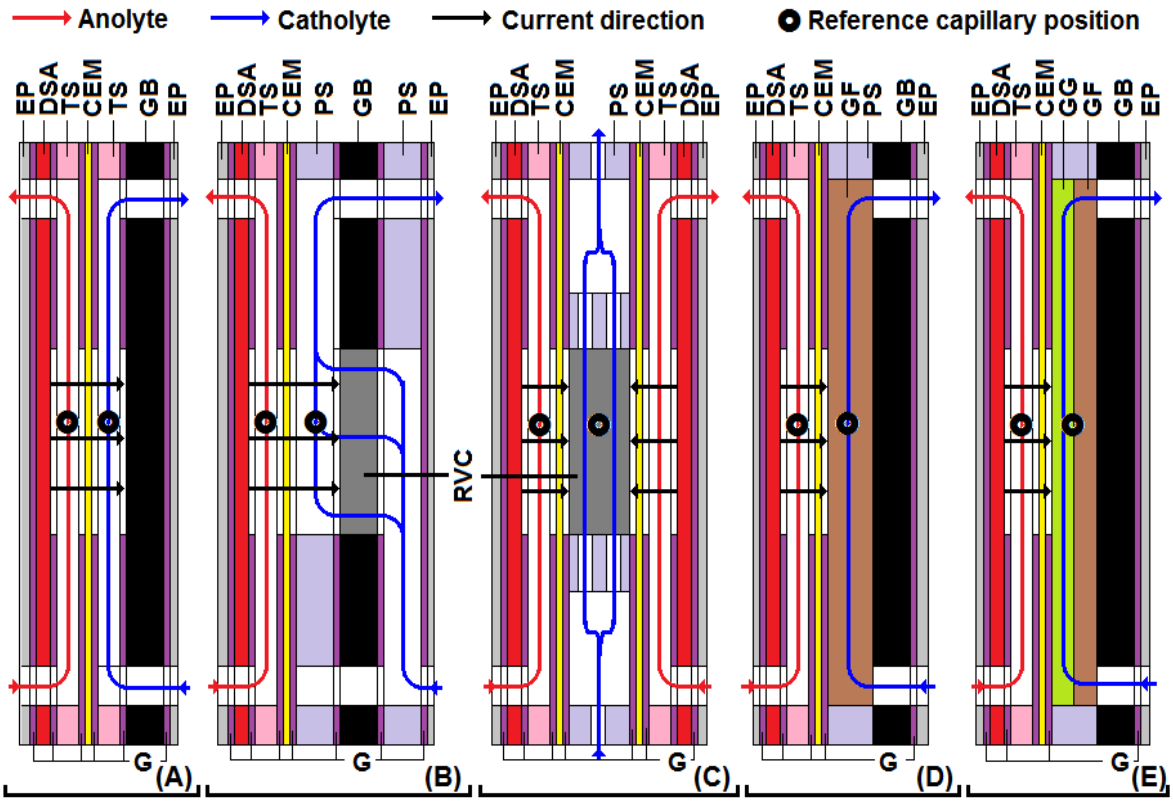

Figura 4.2. Configurations of the FPER based on different cathodic materials: (A) GB; (B) RVC 100 ppi; (C) RVC 500 ppi; (D) GF; (E) RGG. Others components: C.E.M. - cation exchanges membranes, DSA - dimension stable anode, EP - PTFE (Teflon®) end plate, G - rubber gaskets, TS - Teflon® spacers, PS - PMM spacers.

As can be seen from Fig. 4.2, depending on the assembly of the cathode compartment, the electrolyte flow was directed pepependicularly on the applied electric current using GB, RVC 500 ppi, GF and RGG (Fig. 4.2 (A), (C), (D) and (E)) and parallel with electrode surface using RVC 100 ppi (Fig. 4.2 (B)). In all presented configurations, in the anode compartment, the electrolyte flow was directed on the electrode surface, pepependicularly on the applied electric current.

For each tested material, before the HPE experiments, HLV measurements were performed in order to establish the starting conditions for the optimizations studies. For HVL measurements, experimental setup with parts (A) and (B) were used and the electrolyte solution was saturated with O_2 before the measurements started.

For the HPE study, one hour optimization tests and, in some cases, long-term accumulation tests were performed using 100 mL 0.05 M Na_2SO_4. The long-term accumulation tests of HPE were stopped when there was an insignificant increase in the H_2O_2 concentration evaluated using FTHPD.

All experiments were performed at room temperature (≈ 25 °C).

Parameters control at the FPER and FTHPD was performed using a potentiostat/galvanostat and a bi-potentiostat respectively, both piloted by the computer. For equipment control and data acquisition, an application was develop using LabView 2015 software and the experimental data was processed using the ORIGIN 6.1 and Microsoft Excel.

Commercially available materials were used, such as (GB) or sampples from RVC 100 ppi, RVC 500 ppi, GR and RGG were arranged in special assemblies made in the laoratory. RGG, were obtained from graphite bars from depleted Zn-C batteries. The graphite bars were extracted from the batteries, cleaned by washing with water, 48 % H_2SO_4, mix of 48 % H_2SO_4 and 5 % $H_2C_2O_4$ and then were washed with water and distilled water. After washing, the graphite bars were dried at room temperature, crushed and classified by sieving.

The best conditions for the HPE were considered as the optimal compromise between the final concentration of H_2O_2 ($[H_2O_2]_f$), global current efficiency ($C.Ef._G$) and the global electrical energy specific consumption ($W_{S.G}$). In this case, the values obtained for these parameter are global, corresponding to the total duration of the experiments. For the rigorous study of the evolution of the performance parameters of the HPE process over time, a LabView application has been developed that allows to divided data over short duration segments (Δt) and to obtain intermediate values ($[H_2O_2]$, C.Ef, W_S) for the evaluated parameters. The set of results for ($[H_2O_2]_f$, $C.Ef._G$ and $W_{S.G}$ are called *global performance parameters (GPP)* and the set of intermediate results are caled *intermediate performance parameters (IPP)*.

5. HPE study in potentiostatic mode using 2D and 3D carbonaceous materials

In the first stage, was decided the evaluation of performances for HPE in potentiostatic mode of some 3D commercially available carbonaceous materials. The study was started with W.E. made from RVC with porosity of 100 ppi and was continued with RVC 500 ppi, GF, RGG and GB.

5.1. HPE tests using RVC 100 ppi and flow parallel with the current lines

In this case, FPER was equipped with W.E. from RVC 100 ppi and the electrolyte flow was parallel to the electric lines, this flow pattern is illustrated in Fig. 4.2.B. Based on the literature suggestions, in respect with HPE using RVC 100 ppi, the O_2 requirement was provided by continuous air bubbling in the C.T., (see Fig. 4.1 (C1)).

Prior to the HPE tests using W.E. from RVC 100 ppi, the optimal value of working electrode potential ($E_{W.E.}$) was established by HVL measurement at -1 V. Using these starting data, it was decided to perform tests to determine the optimal values of electrolyte (Q_{el}) and (Q_{air}) flow rates and $E_{W.E.}$ for HPE using RVC 100 ppi [57, 58]. The results obtained are presented below.

5.1.2. Optimization of electrolyte flow

To determine the optimum value of Q_{el} for HPE the catholyte solution, saturated with air at room temperature, was circulated through FPER with different flow rates of 4, 8, 20 and 40 mL / min.

Based on the results obtained, it was concluded that the best values for GPP were obtained at Q_{el} of 40 mL/min and the HPE efficiency decreased with the Q_{el} decrease, indicating that the O_2 requirement cannot be provided by saturating with air, at room temperature, of the electrolyte solution prior to the start of the experiments. For this reason, it was decided to continue HPE tests using an air saturated catholyte solution by continuously bubbling it throughout the experiments in the C.T. In this context, tests were performed to determine the optimal value of bubbled Q_{air} in the C.T.

5.1.3. Optimization of air flow

In order to determine the optimal value of the Q_{air}, HPE tests were performed for different values of 20, 40 and 80 mL/min, respectively.

The evolution in time of IPP for each Q_{air} tested value is shown in Fig. 5.3, and the influence Q_{air} on GPP values is presented in Table 5.2

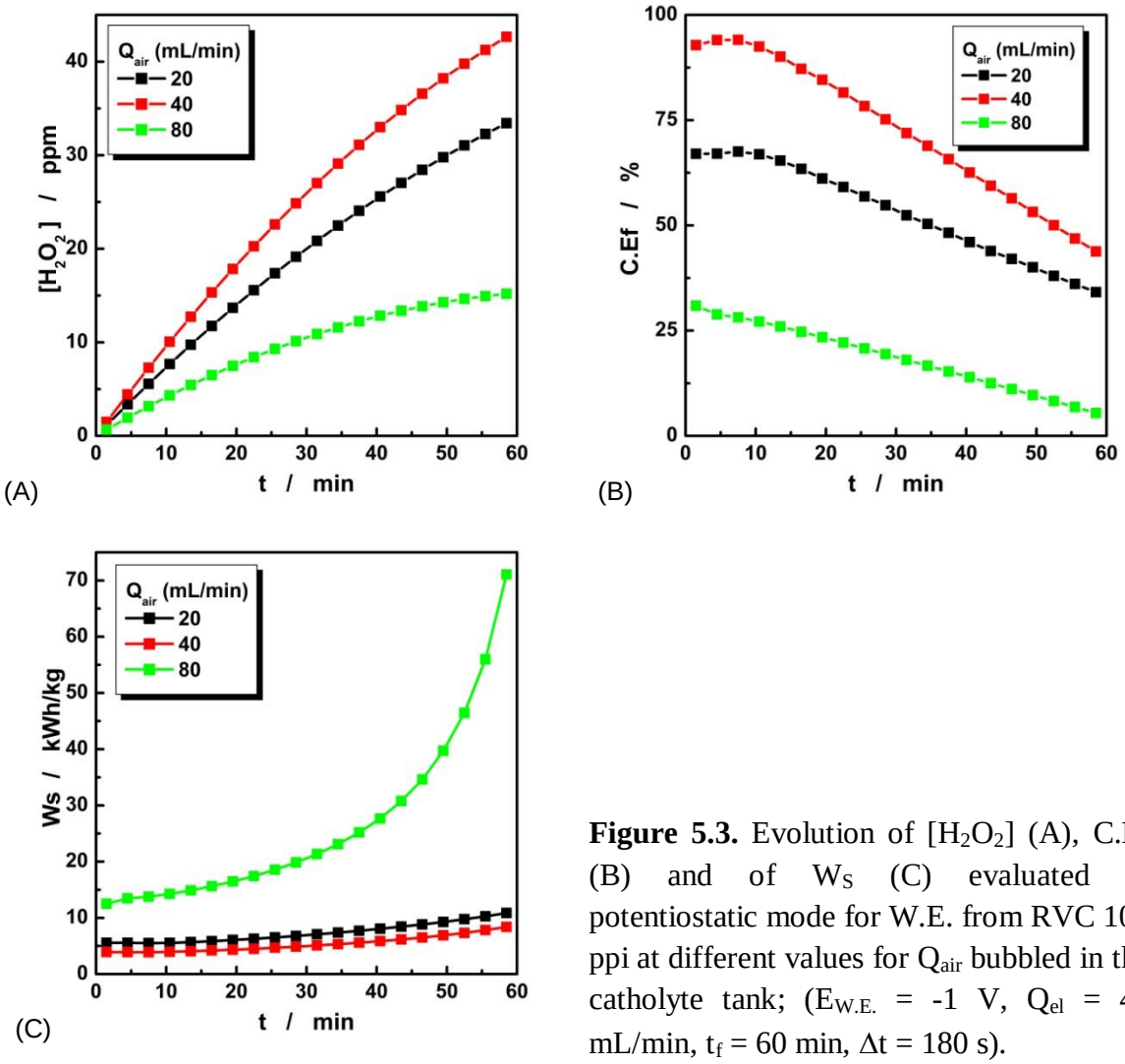

Figure 5.3. Evolution of $[H_2O_2]$ (A), C.Ef (B) and of W_S (C) evaluated in potentiostatic mode for W.E. from RVC 100 ppi at different values for Q_{air} bubbled in the catholyte tank; ($E_{W.E.}$ = -1 V, Q_{el} = 40 mL/min, t_f = 60 min, Δt = 180 s).

Table 5.2. The influence of Q_{air} on GPP evaluated in potentiostatic mode using W.E. from RVC 100 ppi

Q_{el} (mL/min)	**Q_{air} (mL/min)**	**$E_{W.E.}$ (V)**	**$[H_2O_2]_f$ (ppm)**	**$C.Ef_G$ (%)**	**$W_{S.G}$ (kWh/kg)**
40	**20**	-1	34	53	7
	40		43	72	5
	80		15	19	21

By correlating the data from Fig. 5.3 and Table 5.2, it was concluded that the best results are obtained for a Q_{air} value of 40 mL/min. In this case, the highest value for $[H_2O_2]_f$ is obtained with the best $C.Ef._G$ and smaller $W_{S.G}$. The results are much lower for Q_{air} = 20 mL/min and are degraded significantly for Q_{air} = 80 mL/min.

The lower efficiency of HPE at low Q_{air} values (20 mL/min) may be caused by insufficient aeration of the electrolyte solution, which results in a low concentration of

dissolved O_2. This fact, in conjunction with the low conductivity of the electrolyte solution, can cause the uneven distribution of the applied potential in the 3D cathode volume, which can lead to the appearance of areas where a series of secondary reactions are favoured.

Paradoxically, although bubbling air at high flow rates (Q_{air} = 80 mL/min) naturally ensures much more intense aeration of the electrolyte solution, this results in a dramatic degradation of GPP. This phenomenon, reported also in literature [59, 60] but not elucidated yet, may be due to the fact that excessive air bubbling in the C.T. causes the formation of large air bubbles, which rapidly pass through the electrolyte, resulting in a reduced time of contact between air and electrolyte and inefficient aeration. Also, the excess air bubbled, can favour the self-decomposition of H_2O_2, in the volume phase and can lead to H_2O_2 leaving the system in gas form, which would also lead to the degradation of IPP and GPP.

The need and beneficial effects of introducing additional O_2 into the system is confirmed by the results obtained for Q_{air} = 40 mL/min, in which case a much better HPE efficiency was observed when the saturated electrolyte solution with air was passed through the reactor (see Section 5.1.2.).

Next, under the optimal conditions previously established, it was decided to perform optimization of $E_{W.E.}$ value. The results are presented below.

5.1.4. Optimization of applied potential

To establish the optimal value of $E_{W.E.}$ for HPE using W.E. from RVC 100 ppi, different values ranging from -0.8 to -1.4 V were applied. The influence of $E_{W.E.}$ on GPP values is presented in Table 5.3.

Table 5.3. The influence of $E_{W.E.}$ on GPP evaluated in potentiostatic mode using W.E. from RVC 100 ppi

Q_{el} (mL/min)	Q_{air} (mL/min)	$E_{W.E.}$ (V)	$[H_2O_2]_f$ (ppm)	$C.Ef_{.G}$ (%)	$W_{S.G}$ (kWh/kg)
40	40	**-0.8**	21	48	7
		-1.0	43	72	5
		-1.2	45	47	9
		-1.4	39	31	14

Table 5.3 shows that, approximately the same values for $[H_2O_2]_f$ are obtained for $E_{W.E.}$ of -1.0; -1.2 and -1.4 V. Corroborating this result with the values obtained for $C.Ef_{.G}$

and $W_{S.G}$ at all $E_{W.E}$ tested values, it is obvious that the best value of $E_{W.E}$. for HPE is -1.0 V. At this value are obtained the best values for C.Ef.$_G$ and $W_{S.G}$. Based on these results, it was concluded that $E_{W.E.}$ = -1.0 V represents the optimum value for HPE using W.E. from RVC 100 ppi.

IPP evolution at different values of $E_{W.E.}$ (-0.8; -1.0; -1.2 respectively -1.4 V) is shown in Fig. 5.4.

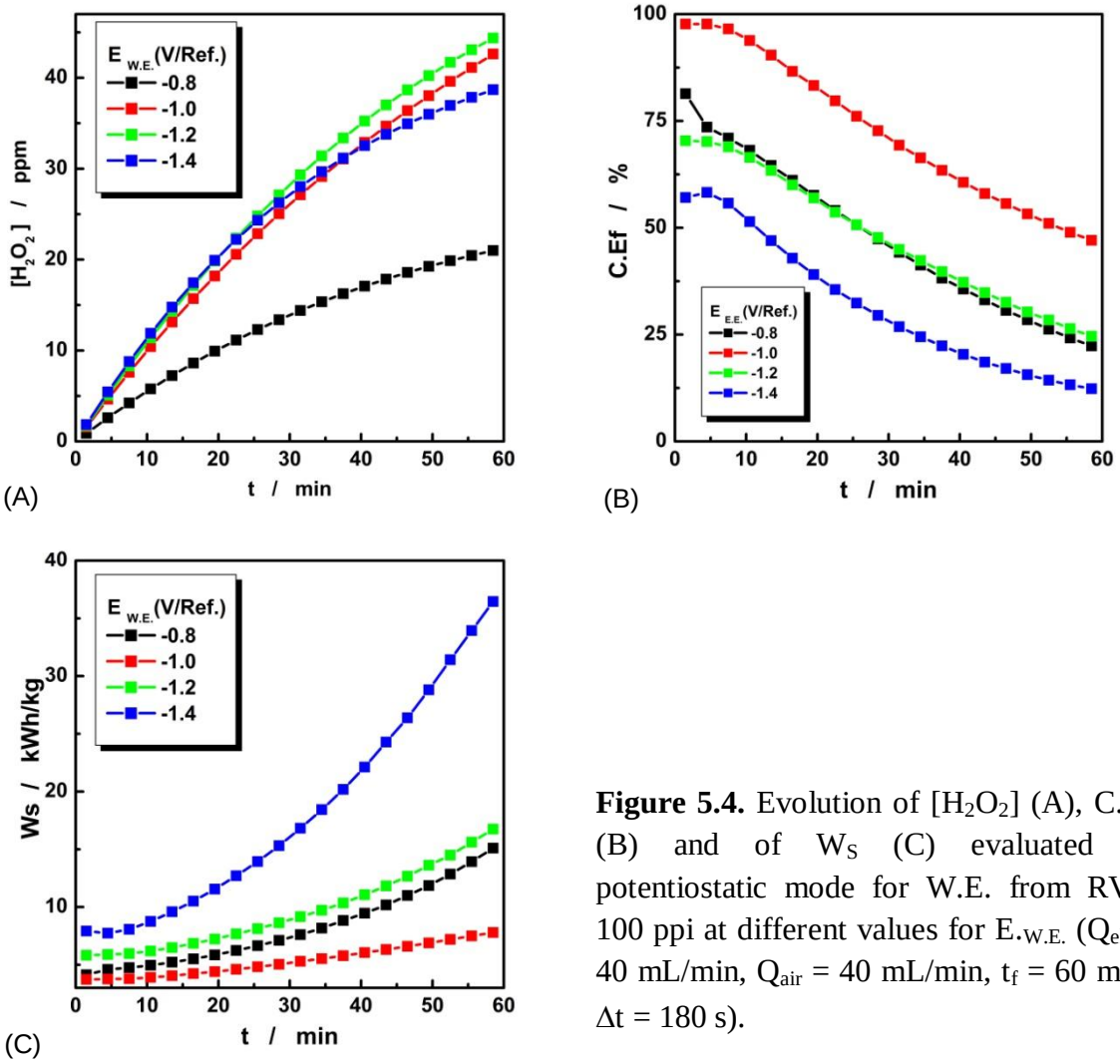

Figure 5.4. Evolution of $[H_2O_2]$ (A), C.Ef (B) and of W_S (C) evaluated in potentiostatic mode for W.E. from RVC 100 ppi at different values for $E._{W.E.}$ (Q_{el} = 40 mL/min, Q_{air} = 40 mL/min, t_f = 60 min, Δt = 180 s).

Fig. 5.4 shows that the evolution in time of $[H_2O_2]$ at -1.0; -1.2 and -1.4 V is almost identical, C.Ef reaches maximum values at the beginning of the experiment and decreases continuously during the tests and W_S increases continuously, reaching maximum values at the end of the experiments.

Following the performed tests (according to sections 5.1.2 ÷ 5.1.4), it was established that for the exploitation of W.E. made from RVC 100 ppi for HPE, the optimum conditions are: Q_{el} = 40 mL/min, Q_{air} = 40 mL/min and $E_{W.E.}$ = -1.0 V. In these conditions, it was decided to perform a HPE long-term accumulation test. Evolution of [H_2O_2] was observed by FTHPD, and the experiment was stopped when the recorded current by D.E. ($I_{D.E.}$) has slowly increased, indicating an insignificant increase of accumulated [H_2O_2].

During the long-term accumulation test, it was observed that [H_2O_2] increases significantly during the first 3 h of the experiment, followed by a small increase and an approximately constant value at the end. Correspondingly, C.Ef has a maximum value at the beginning of the HPE test and then decreases to very low values at the end of it. W_S increases continuously throughout the experiment, reaching enormous values at the end.

At the end of the long-term accumulation test, $[H_2O_2]_f$ reaches a value of 52 ppm, with a $C.Ef_{.G}$ of 18% and a $W_{S.G}$ of 21 kWh/kg. $[H_2O_2]_f$ obtained in the accumulation regime for 4h is not much higher than that obtained for 1h under the same conditions ($[H_2O_2]_f$ = 43 ppm), indicating that the long-term test of the HPE does not have a beneficial effect on the GPP of the process.

The unsatisfactory results obtained in the long-term accumulation test can be caused by the passivation of the electrode surface, the type of uncontrolled flow of the electrolyte, the decomposition of H_2O_2 caused by air bubbling in the C.T. and by favouring secondary reactions.

Another important aspect that can significantly influence the efficiency of HPE is the flow velocity of the electrolyte (u), expressed as the ratio between Q_{el} and the area of the electrolyte flow section (A_s). In relation to this parameter, in order to obtain the same performances at the industrial level, it is necessary to maintain the ratio between Q_{el} and A_s equal to that used at the experimental level. To meet this goal, considering that in the case of W.E from RVC 100 ppi the electrolyte flow is parallel with the electric field, increasing the electrode surface in an industrial application would require a proportional increase of Q_{el} to exaggerated values. In addition, the combination of a large RVC electrode and very large flow rates could cause serious problems with the electrode's mechanical resistence.

Considering the promising results obtained using W.E. from the RVC 100 ppi and from the desire to solve a large part of the deficiencies detected, it was decided to design, build and test a new model of 3D W.E. for HPE based on RVC, to ensure an electrolyte

flow perpendicular to the electric field lines. For this purpose, a sample of RVC 500 ppi was used. The new configuration allows the electrolyte to flow through a smaller section, along the electrode, through its pores.

Further, HPE tests were performed in potentiostatic mode using W.E. from RVC 500 ppi. The results obtained are presented in the following.

5.2. HPE tests using RVC 500 ppi and perpendicular flow to the current lines

For HPE tests using RVC 500 ppi, the electrolyte was directed to flow through the pores of this material, perpendicular to the electric field lines. In addition, to counter the disadvantages identified when the electrolyte oxygenation was achieved by air bubbling in the C.T., it was decided to use a three-phase system (solid-liquid-gas). This is presented as an efficient alternative for increasing the performance of the HPE process [61-66]. Specifically, it was decided to inject air into the catholyte flow followed by the introduction of the air-electrolyte mixture into the FPER.

To perform measurements using W.E. from RVC 500 ppi, the experimental setup presented in Fig. 4.1 with the arrangement (C2) was used and the electrolyte flow is shown in Fig. 4.2. (C).

Prior to HPE tests, HVL measurements were made using RVC 500 ppi and the $E_{W.E.}$ of -0.8 V and Q_{el} 40 mL/min were established as optimal. Using these optimal values, it was decided to carry out a new set of tests to optimize Q_{air} and $E_{W.E.}$ using W.E. from RVC 500 ppi. The results are presented below.

5.2.2. Optimization of air flow

To determine optimal Q_{air} for HPE using W.E. from RVC 500 ppi different values of this parameter were tested. The evolution in time of IPP is illustrated in Fig. 5.7 and the GPP obtained values for each tested value of Q_{air} are presented in Table 5.4.

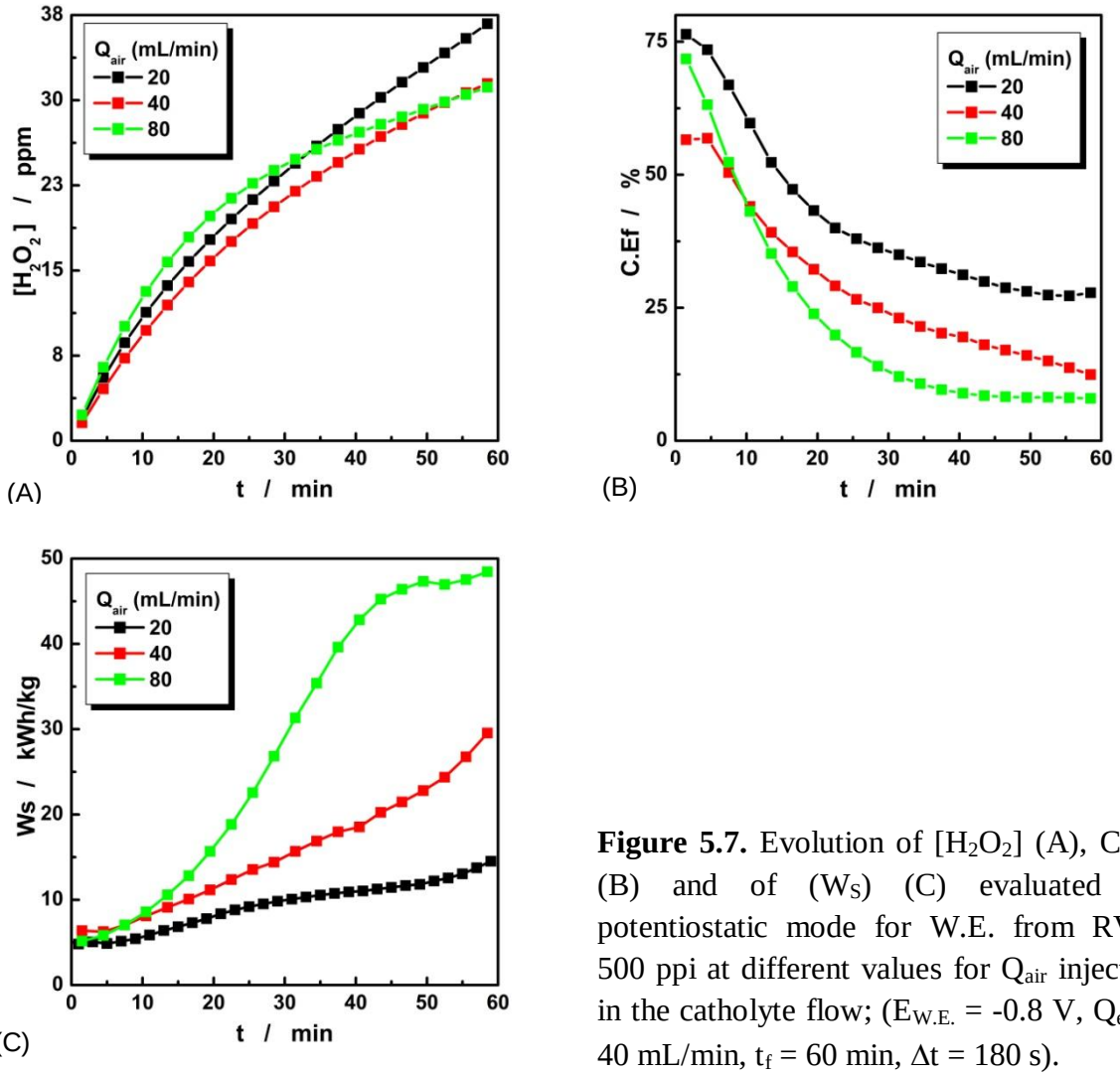

Figure 5.7. Evolution of $[H_2O_2]$ (A), C.Ef (B) and of (W_S) (C) evaluated in potentiostatic mode for W.E. from RVC 500 ppi at different values for Q_{air} injected in the catholyte flow; ($E_{W.E.}$ = -0.8 V, Q_{el} = 40 mL/min, t_f = 60 min, Δt = 180 s).

Table 5.4. The influence of Q_{air} on GPP evaluated in potentiostatic mode for W.E. from RVC 500 ppi

Q_{el} (mL/min)	**Q_{air} (mL/min)**	**$E_{W.E.}$ (V)**	**$[H_2O_2]_f$ (ppm)**	**$C.Ef_G$ (%)**	**$W_{S.G}$ (kWh/kg)**
40	**20**	-0.8	40	45	8
	40		32	28	13
	80		24	19	20

By correlating the data in Fig. 5.7 with those from Table 5.4 it is observed that the best results were obtained for a Q_{air} value of 20 mL/min. For this value of Q_{air} the highest $[H_2O_2]_f$ is obtained, with a good $C.Ef._G$ and a small $W_{S.G}$. At higher Q_{air} values (40 and 80 mL/min) the obtained results are less satisfactory.

Based on the above presented results, it was established that the Q_{air} value of 20 mL/min is considered optimal for HPE using W.E. from RVC 500 ppi. This value,

representing half of the best value of Q_{air} evaluated for W.E. from RVC 100 ppi, indicates a more efficient oxygenation of the electrolyte by injecting air into the catholyte stream compared with the aeration by bubbling the air into the C.T. Operating the three-phase system can halve the costs required to pump air into the system.

The decrease of HPE efficiency at high Q_{air} values (40, 80 mL/min) may be caused by blocking the electrode surface due to the presence of large air bubbles in the electrolyte flow. Large air bubbles can adhere to the surface of the electrode and thus can block the active surface of the electrode, leading to decreased HPE efficiency.

Further, using the optimal Q_{air} value established from this set of measurements, $E_{W.E.}$ optimization tests were performed for W.E. from RVC 500 ppi.

5.2.3. Optimization of applied potential

To establish the optimal value of $E_{W.E.}$ for HPE using W.E. from RVC 500 ppi, tests were performed at different values, ranging from -0.4 to -1.0 V. For each applied value of $E_{W.E.}$, the influence of $E_{W.E.}$ on GPP is presented in Table 5.5. and the evolution in time of IPP is shown in Fig. 5.8.

Table 5.5. The influence of $E_{W.E.}$ on GPP evaluated in potentiostatic mode using W.E. from RVC 500 ppi

Q_{el} (mL/min)	**Q_{air} (mL/min)**	**$E_{W.E.}$ (V)**	**$[H_2O_2]_f$ (ppm)**	**$C.Ef_G$ (%)**	**$W_{S.G}$ (kWh/kg)**
40	20	**-0.4**	2	8	36
		-0.6	28	48	7
		-0.7	28	32	11
		-0.8	40	45	8
		-1.0	17	12	35

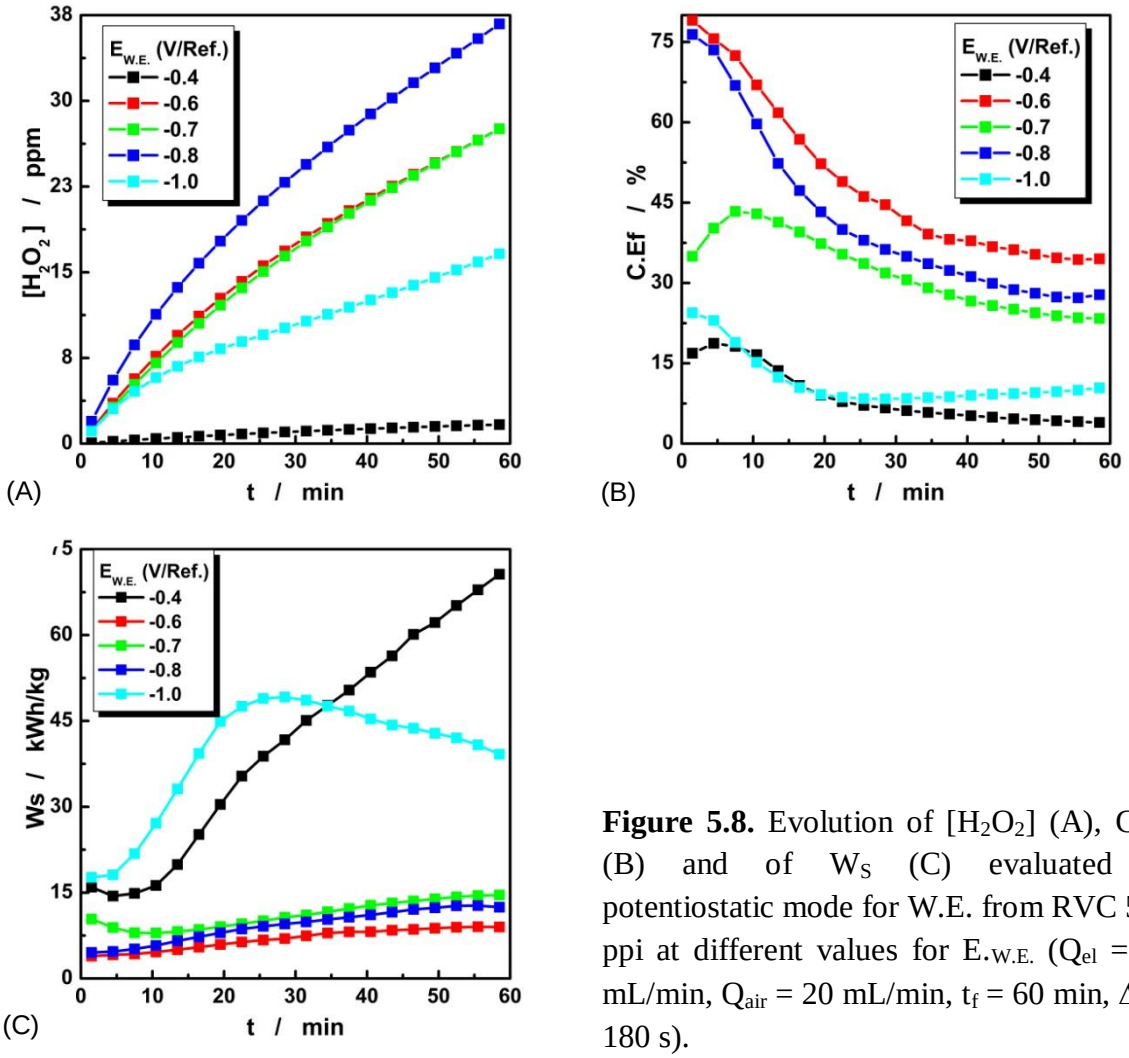

Figure 5.8. Evolution of $[H_2O_2]$ (A), C.Ef (B) and of W_S (C) evaluated in potentiostatic mode for W.E. from RVC 500 ppi at different values for $E._{W.E.}$ (Q_{el} = 40 mL/min, Q_{air} = 20 mL/min, t_f = 60 min, Δt = 180 s).

Fig. 5.8 and Table 5.5 shows that the highest $[H_2O_2]_f$ is obtained for $E_{W.E}$ = -0.8 V. At $E_{W.E}$ = -0.7 and -0.6 V, $[H_2O_2]_f$ obtained is equal in both cases (28 ppm). The lowest productivity, almost zero, is obtained for $E_{W.E}$ = -0.4 V. This value was confirmed from HVL measurements as an inefficient value for HPE.

The small $[H_2O_2]_f$ obtained for $E_{W.E}$ = -1 V indicates that excessive polarization of W.E. can lead to favouring of parasitic processes, with negative effects on the HPE process. With respect to $C.Ef._G$ and $W_{S.G}$, similar results were obtained for $E_{W.E.}$ values of -0.6; -0.7 and -0.8 V. The highest values of $W_{S.G}$, of about 35 kWh/kg, were obtained for $E_{W.E.}$ values of -0.4 and -1.0 V, the causes being the same ones which also determined a low productivity in these cases. Taking into account the maximum productivity obtained, it was established that for W.E. from RVC 500 ppi, operated in potentiostatic mode and using the three-phase system, the optimum value for $E_{W.E}$ is -0.8 V. Having established the

optimal values for Q_{el}, Q_{air} and $E_{W.E.}$, it was further decided to study HPE using W.E. of RVC 500 ppi in accumulation mode for a longer time.

The long-term study of HPE in accumulation mode using W.E. from RVC 500 ppi was performed under the optimal conditions previously established (Q_{el}, = 40 mL/min, Q_{air} = 20 mL/min and $E_{W.E.}$ = -0.8 V) for 2h. It was decided to stop the experiment when there was an insignificant increase of $I_{E.D.}$ to avoid decreasing of $C.Ef._G$ and exaggerated increase of $W_{S.G}$.

During the long-term accumulation test it was observed that $[H_2O_2]$ increases continuously over time, C.Ef reaches a maximum value at the beginning of the HPE test and decreases to very low values towards the end of it. Ws continuously increase throughout the HPE test in long-term accumulation.

At the end of the long-term accumulation test, $[H_2O_2]_f$ reaches a value of 42 ppm. This productivity is achieved with a $C.Ef._G$ = 16% and a $W_{S.G}$ = 22 kWh/kg. $[H_2O_2]_f$ obtained in the accumulation mode for 2h is almost equal to that obtained for 1h, ($[H_2O_2]_f$ = 40 ppm), under the same experimental conditions with much better values for C.Ef and $W_{S.G}$ ($C.Ef._G \approx 45\%$ and $W_{S.G} \approx 8$ kWh / kg).

Based on the results presented above, it was found that the rate of accumulation of H_2O_2 after 1h of recirculation the electrolyte solution becomes insignificant. Because of this, low concentration is achieved, which leads to low values for $C.Ef._G$ and high values for $W_{S.G}$.

It was considered that the unsatisfactory results obtained in long-term accumulation regime using W.E. from RVC 500 ppi were also caused by the way the necessary of O_2 is provided. Thus, by simply injecting air into the electrolyte stream, large gas bubbles can form and block the electrode surface.

5.3. HPE tests in potentiostatic mode using W.E. from GF, RGG and GB

In order to obtain comparative data, it was attempted to study the HPE process in potentiostatic mode, using W.E. made from GF, RGG and GB. Unfortunately, during the tests performed with W.E. from GF and RGG, it has been found that operating HPE in potentiostatic mode is quite difficult if air is injected continuously into the catholyte stream. Practically, under these experimental conditions, the transport of large air bubbles through the 3D electrode led to the blocking of the Luggin capillaries that make the

connection with the reference electrodes, thus leading to the impossibility of a rigorous control of the potential applied at the W.E. and the process. For this reason, it was decided to continue the study on HPE using W.E. from GF and RGG only in galvanostatic mode.

Using W.E. from GB, at values established by HVL measurements, a test was performed at $E_{W.E.}$ -0.7 V and Q_{air} = 10 mL/min. Under these conditions, $[H_2O_2]_f$ = 7 ppm was obtained with $C.Ef._G$ = 52% and $W_{S.G}$ = 5 kWh/kg. Due to the very low productivity obtained in this case, the optimization studies in potentiostatic regime were not continued using this type of material.

Even if the results obtained in potentiostatic mode using E.L. from RVC 100 ppi are better than those obtained using E.L. from RVC 500 ppi, the EAO study was continued using CVR 500 ppi (hereinafter referred to as CVR) due to the possibilities of electrolyte flow that this material presents.

6. HPE study in galvanostatic mode using different carbonaceous materials

In order to produce H_2O_2 with the lowest costs, it was decided to test the possibility of using recycled materials for HPE. In this context, in order to evaluate the feasibility of their use, it was decided to compare the performances of the recycled materials with those of commercial carbonaceous materials, intensively studied for HPE [58].

In the first step, different 2D and 3D cathode materials, commercially available and recycled were selected. Of the commercially available materials, GB was chosen for the 2D electrode and RVC 500 ppi (called RVC) and GF for the 3D electrodes. As a recycled carbonaceous material, RGG was used.

Prior to HPE tests using the selected materials, to prevent the introduction of large bubbles in FPER by simply injecting air into the catholyte stream, it was decided to use a device to ensure the fine dispersion of air bubbles in the electrolyte. In this case, a centrifugal pump with the role of air-water mixer (A.W.M.) was introduced in the experimental setup (Section (C2) and (C3) of Fig. 4.1.C). With the help of A.W.M. an emulsion, obtained by the fine dispersion of air bubbles in the electrolyte solution, is introduced into the FPER.

Subsequently, the study of HPE in galvanostatic mode was started using the cathode materials selected from the commercially available carbon materials.

6.1. HPE test using commercial avalaible carbonaceous materials: GB, RVC and GF

Prior to HPE tests using W.E. made from commercially available carbonaceous materials, HVL measurements were performed in order to obtain the starting values for the optimization tests for each selected material. Thus, for W.E. from GB, RVC and GF, the starting values of $I_{W.E.}$ were -2, -15 and -40 mA respectively.

With the starting data set for each selected material, it was decided to carry out optimization tests of the HPE process.

6.1.2. Optimization of HPE process using GB, RVC and GF

During these tests, the influence of Q_{air} on HPE was studied using W.E. from RVC and GF and the influence of $I_{W.E.}$ was studied using W.E. from RVC. Basically, HPE tests were performed at Q_{air} values between 10 and 80 mL/min (for RVC) and between 10 and 40 mL/min (for GF). During all HPE test, the introduction of air into the system was performed as indicated in Fig. 4.1.C, using sections (C2) and (C3) simultaneously. For each of the 3 selected materials, HPE studies started from the values of $I_{W.E.}$ established by HVL.

The operating conditions for the HPE tests performed with each type of material and the results obtained for the GPP are presented in Table 6.1

Table 6.1. HPE optimization tests using W.E. from GB, RVC and GF in galvanostatic mode and the results obtained for GPP

Cathode material	$I_{W.E.}$ (mA)	Q_{air} (mL/min)	$[H_2O_2]_f$ (ppm)	$C.Ef_{.G}$ (%)	$W_{S.G}$ (kWh/kg)
GB	-2	10	7	57	5
RVC	**-12,5**	**20**	61	76	7
	-15	**10**	73	76	6
		20	73	76	7
		40	71	74	7
		80	69	72	6
GF	-40	**10**	124	49	8
		20	111	43	9
		40	128	50	8

As can be seen from Table 6.1, using the original aeration system, A.W.M., the Q_{air} value has a small influence on the efficiency of the HPE process. Basically, the results obtained for GPP using W.E. from RVC and GF does not change significantly depending on the Q_{air} tested value. For HPE using W.E. from GF, the optimal value of Q_{air} was considered 40 mL/min. At this value, the best results were obtained for $[H_2O_2]_f$ and $C.Ef._G$. From the RVC, the results obtained are very close. In this case, the lowest tested value of Q_{air} (10 mL/min) was established as optimal, because it involves the lowest costs associated with providing the O_2 requirement.

The influence of the $I_{W.E.}$ on HPE using W.E. from RVC was tested at Q_{air} = 20 mL/min and it was found that the results obtained for $C.Ef._G$ and $W_{S.G}$ are practically identical, but productivity is higher if the value of $I_{W.E.}$ is higher (-15 mA). For this reason, -15 mA is considered as optimal.

Taking into account the extremely low productivity of W.E. from GB, the study of the Q_{air} influence on the HPE was abandoned. For GB, one comparative experiment being performed galvanostatic mode, at Q_{air} = 10 mL/min and $I_{W.E.}$ = -2 mA.

Following HPE tests using W.E. from GB, RVC and GF, it was found that the highest productivity was obtained using W.E. from GF (128 ppm). However, even if the highest productivity was achieved using W.E. from GF, the most efficient material for HPE was considered RVC due to the obtained values for $C.Ef._G$ and $W_{S.G}$.

Increasing of HPE efficiency due to the introduction of air in the form of fine bubbles, using the A.W.M. is confirmed by the higher productivity obtained using W.E. from RVC (71 ppm) to that obtained in potentiostatic mode (≈ 40 ppm).

Based on result presented above, the HPE study was carried out in the accumulation mode using RVC at the optimal operating parameters previously established (Q_{air} = 10 mL/min, $I_{W.E.}$ = -15 mA). The duration of the long-term accumulation study of HPE was almost 6 hours.

During the accumulation test performed in this case, it was observed that the tendency of capping of the curve indicating H_2O_2 production is much lower than in the case of potentiostatic tests. In addition, C.Ef decreases and W_S increases in time, but these parameters remain at acceptable values (C.Ef over 50% and Ws around 9 kWh/kg) for approximately 3h.

At the end of the long-term accumulation test, after 6h, $[H_2O_2]_f$ reaches a value of 278 ppm, with a $C.Ef._G$ of 49% and $W_{S.G}$ of 9 kWh/kg.

These results obtained in galvanostatic mode using W.E. from RVC are more promising than those obtained in potentiostatic mode using the same type of material.

Based on the results obtained from the long-term accumulation test, it is confirmed once again that the improvements made, regarding the air introduction in system and the galvanostatic operation, are beneficial for increasing the efficiency of the HPE process in the accumulation regime even for long term.

After performing the optimization and accumulation tests performed using commercial carbon materials, it was decided to test the RGG. The carried tests and the obtained results using this type of material are presented next.

6.2. HPE tests using recycled carbonaceous material: RGG

For the HPE tests using RGG, the W.E. was made from granules with a diameter between 0.60 mm and 2 mm, obtained by crushing some graphite bars recovered from the used Zn-C batteries.

Before performing HPE tests using W.E. from RGG, the value of -20 mA was selected for $I_{W.E.}$ by HVL. At this value, using a series of 3D electrodes made from RGG, several optimization tests for $I_{W.E.}$, Q_{air} and RGG dimensions were performed. During all these tests, the oxygenation of the catholyte was performed using the original aeration system, A.W.M.

6.2.2. Optimization of HPE process using RGG

The conditions for the optimization tests using W.E. from the RGG and the obtained results for the GPP are presented in Table 6.2

Table 6.2. HPE optimization tests of $I_{W.E.}$ and Q_{air} using W.E. from RGG in galvanostatic mode and the results obtained for GPP

Cathode material	**$I_{W.E.}$ (mA)**	**Q_{air} (mL/min)**	**$[H_2O_2]_f$ (ppm)**	**$C.Ef_{.G}$ (%)**	**$W_{S.G}$ (kWh/kg)**
RGG (0.6<d<2 mm)	**-10**	10	34	53	5
	-20		41	33	10
	-30		41	22	17
	-40		50	19	21
	-40	**20**	38	15	28

It can be seen from Table 6.2, that similar results are obtained with respect to $[H_2O_2]_f$ at Q_{air} = 10 mL/min for values of $I_{W.E.}$ of -20; -30 and -40 mA, but $C.Ef._G$ is decreasing, reaching values of 33, 22 and 19%, respectively. Accordingly, $W_{S.G}$ increases with increasing the applied $I_{W.E.}$ value and reaches the highest values at $I_{W.E.}$ = -40 mA ($W_{S.G}$ = 21 kWh/kg). The best results for W.E. from RGG are obtained at Q_{air} = 10 mL/min and $I_{W.E.}$ = -10 mA.

Based on the results presented in Table 6.2, it is found that an increase of Q_{air} does not lead to an increase of HPE efficiency. On the contrary, the results obtained for the same value of I $I_{W.E.}$ ($I_{W.E.}$ = -40 mA) and different Q_{air} are less satisfactory at higher flow rates. At Q_{air} = 20 mL/min, the results obtained are weaker than those obtained at Q_{air} = 10 mL/min.

In the next step, it was decided to test the influence of the RGG dimensions on the HPE [67]. In this case, it was decided to perform HPE tests using RGG with diameters between 0.5 <d <1.0 mm; 1.0 <d <2.0 mm and 2.0 <d <3.0 mm. The GPP values obtained for each range of tested diameters, at different times of the experiments, are presented in Table 6.3.

Table 6.3. The influence of the RGG diameter on the GPP evaluated in galvanostatic mode

Crt. nr.	**Diameter RGG (mm)**	**$I_{W.E.}$ (mA)**	**t (min)**	**$[H_2O_2]_f$ (ppm)**	**$C.Ef._G$ (%)**	**$W_{S.G}$ (kWh/kg)**
1	**2.0 < d < 3.0**	-10	30	18	55	5
2	**1.0 < d < 2.0**			15	48	6
3	**0.5 < d < 1.0**			12	37	8
4	**0.6< d < 2.0**	-10	60	34	53	5
5	**2.0 < d < 3.0**			27	42	7

As can be seen from the first 3 rows of Table 6.3, in the short duration tests (30 min.), the best results regarding GPP were obtained using RGG with a diameter between 2 and 3 mm. At the same time, the lowest efficiency was obtained when granules with a diameter of 0.5 <d <1.0 mm were used. The decrease of the efficiency of the HPE process together with the decrease of the RGG diameter can be explained by the formation of a compact RGG layer in which preferential electrolyte flow channels are formed. At the same time, this compact layer can have a strong shielding effect, causing an extremely uneven distribution of the potential in the 3D electrode volume. In the case of large-size

RGG diameter (2 <d <3 mm), a uniform flow of the electrolyte is ensured through the electrode layer but its effective working surface is reduced, resulting in a reduction in the efficiency of the HPE process.

Based on the data in lines 4 and 5 of Table 6.3 we can compare the efficiency of the HPE process for W.E. from RGG with dimensions between 2 and 3 mm with that of W.E. from RGG with dimensions between 0.6 and 2 mm. In these cases, the best results regarding GPP were obtained using RGG with a diameter between 0.6 and 2 mm. This increased efficiency may be due to the fact that, by using non-uniform dimensions, both a uniform flow of the electrolyte through the RGG layer and a large working electrode surface are ensured.

6.2.3. Test of HPE in long-term accumulation mode using W.E. from RGG

Long-term HPE study using W.E. from RGG was performed a optimal conditions previously established (Q_{air} = 10 mL/min and $I_{W.E.}$ = -10 mA, RGG with a diameter between 0.6 and 2 mm), for a duration of ≈ 2 h.

At the end of the long-term accumulation test, $[H_2O_2]_f$ reaches a value of 57 ppm, with $C.Ef._G$ of 41% and a $W_{S.G}$ of 7 kWh/kg. Productivity obtained in long-term accumulation test using W.E. from RGG is improved compared to the 1h accumulation study, but the results regarding $C.Ef._G$ and $W_{S.G}$ it is obviously degrading.

After all experimental measurements with selected materials, the comparative presentation of the obtained results was made and, implicitly, the comparative evaluation of the performance of the materials tested in relation to the HPE process.

6.3. Comparison between the results obtained in galvanostatic mode using the 4 materials

The results obtained after 1h of HPE in accumulation mode for each the tested materials (GB, RVC, GF and RGG) are presented next [68]. The evolution of IPP for the 4 cathode materials tested is shown in Fig. 6.6.

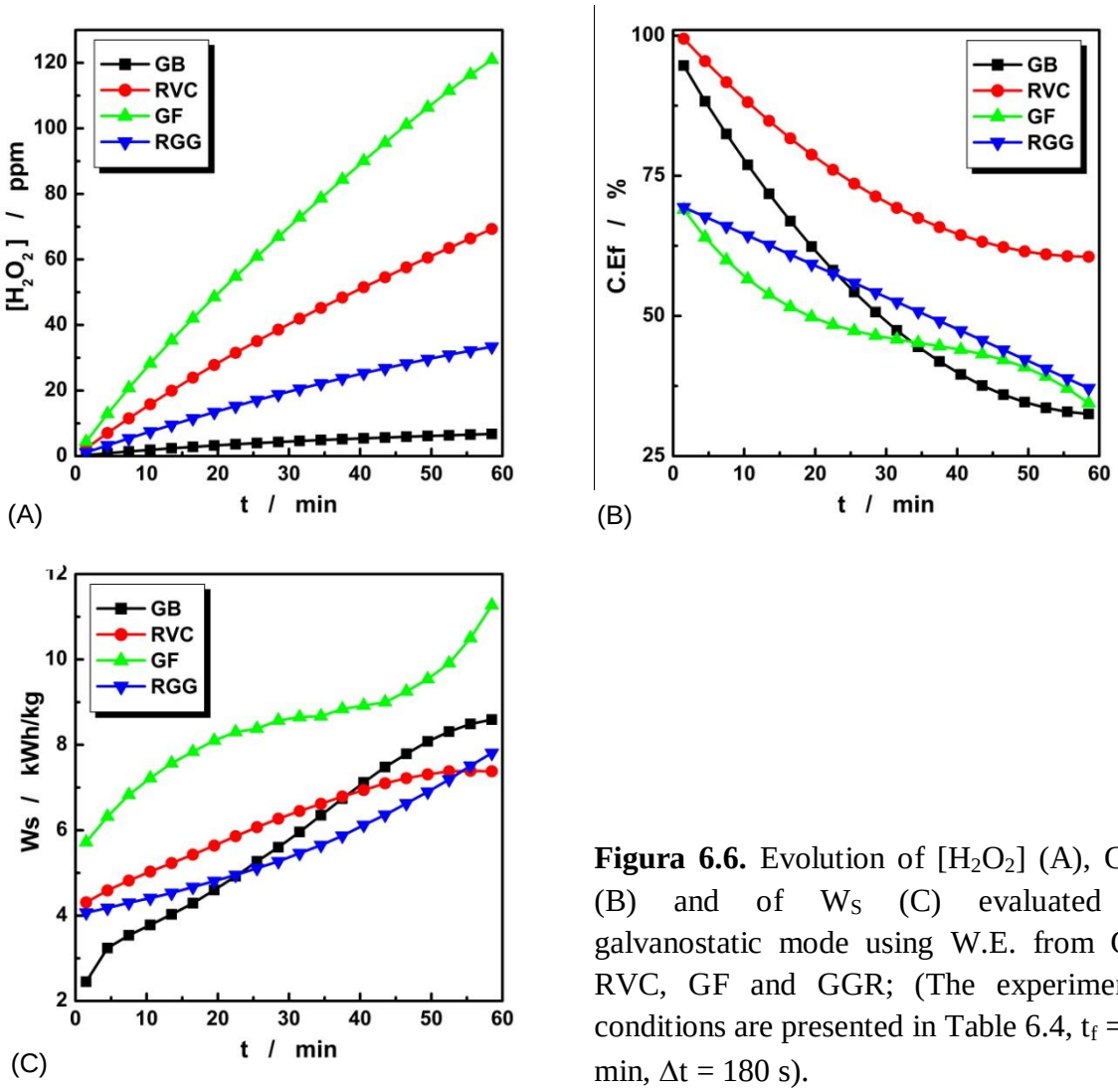

Figura 6.6. Evolution of $[H_2O_2]$ (A), C.Ef (B) and of W_S (C) evaluated in galvanostatic mode using W.E. from GB, RVC, GF and GGR; (The experimental conditions are presented in Table 6.4, t_f = 60 min, Δt = 180 s).

As can be seen from Fig. 6.6 (A), W.E. from GF ensures the best productivity, being followed by those made from RVC and RGG. The lowest productivity is obtained using W.E. from GB.

From Fig. 6.6 (B) it is observed that the best C.Ef values are obtained using W.E. from RVC. In this case, C.Ef starts from ~ 100% and decreases continuously up to 60% at the end of the test. For W.E. from GF and RGG, C.Ef reaches a maximum value at the beginning of the experiment and decreases considerably over time, reaching small values, below 40%. The most pronounced decrease in C.Ef is recorded when using W.E. from GB.

From Fig. 6.6 (C) it can be observed that the highest W_S is obtained using W.E. from GF. The W_S for the other 3 tested materials vary in time in almost similar way.

The optimal conditions established for the 4 tested materials and the GPP values obtained are presented in Table 6.4.

Table 6.4. GPP values obtained in optimal conditions for each material tested

Cathode material	$I_{W.E.}$ (mA)	Q_{air} (mL/min)	$[H_2O_2]_f$ (ppm)	$C.Ef._G$ (%)	$W_{S.G}$ (kWh/kg)
GB	-2	10	7	57	5
RVC	-15	10	73	76	6
GF	-40	40	128	50	8
RGG	-10	10	34	53	5

Comparing the obtained values for GPP using each tested material, presented in Table 6.4, it is observed that, using W.E. from GB, was obtained the best $W_{S.G}$ and a satisfactory $C.Ef._G$, but in this case, was also obtained the lowest productivity. At the industrial level, the use of GB would require the use of huge reactors to ensure an electrode surface suitable for increased productivity.

RVC seems to be the most effective material for HPE, which ensures satisfactory productivity, good $C.Ef._G$ and low $W_{S.G}$. Unfortunately, the use of RVC at the industrial level is difficult due to its fragility and high price.

Using W.E. from GF, the highest productivity is obtained, but in this case, the efficiency is reduced, obtaining the highest value for $W_{S.G}$ and the lowest value for $C.Ef._G$.

RGG presents satisfactory results, especially in relation to $C.Ef._G$ and $W_{S.G}$. Productivity is not very high in this case, but compared to the commercially available and widely used materials for HPE, the results obtained using this type of material are considered extremely promising. Based on the results presented above, is concluded that RGG can provide a cheap alternative to the 3D available carbonaceous materials for HPE.

The results obtained in the present work are comparable to those obtained under similar conditions in other works presented in the literature [20, 23, 33, 69, 70].

For a more efficient comparison of the RGG and RVC performances, HPE tests are performed, in the long term accumulation tests (2h), using W.E. from RGG and RVC at optimal parameter established for each material. By comparing the results obtained using the two materials, it was found that the productivity obtained using W.E. from the RVC is double compared to that obtained when RGG is used, but it must be taken into account that $I_{W.E.}$ is 50% higher in the case of RVC. The values obtained for $C.Ef._G$ are comparable and those obtained for $W_{S.G}$ are practically identical.

The use of RGG allows carrying out electroactivation tests of the surface W.E. In this context, using RGG galvanostatic electroactivation tests were performed

6.5. RGG electroactivation test in galvanostatic mode by auto-adaptative techniques

It was decided to test the possibilities of *in situ* electroactivation (ISEA) of RGG using the auto-adaptive current technique [71] using a three-step protocol: *(I) HPE, (II) anodizing and (III) partial reduction.*

With the activation protocol established, a series of tests were performed to determine the influence of the limiting potentials imposed for oxidation and reduction step on the efficiency of the activation protocol. The latter was estimated based on the current $I_{E.D.}$ registered with the help of DAFAO.

Following the tests carried out, it was concluded that, regardless of the electrical parameters imposed during the ISEA protocol, the attempts to increase the efficiency of the HPE have failed.

In the context presented above and based on the literature data [72], it was decided to improve the activation protocol by introducing an additional stage within it. This new step, generically called "washing", involves disconnecting W.E. after applying the anodizing and partial reduction steps for a predetermined period of time. At the same time, during the new washing step, the electrolyte is further pumped through FPER.

By applying this new activation protocol, promising results have been obtained in terms of maintaining constant and even increasing the value of $I_{D.E.}$ recorded at the end of the production stages. In this context, it was decided to study the influence of the duration of the production stage and the washing stage on the efficiency of HPE. The values of the electrical and/or time parameters for each step and the results obtained for each test performed are presented in Table 6.9.

Table 6.9. The influence of the duration of the production and the washing stage on HPE

Step I		Step II		Step III		Step IV	Cycle 1	Cycle 5	$I_{E.D.}$ Evolution
$I_{W.E.}$ (mA)	t (s)	$I_{W.E.}$ (mA)	$E_{W.E.\ max.}$ (V)	$I_{W.E.}$ (mA)	$E_{W.E.\ min.}$ (V)	t (s)	$I_{D.E.}$ (μA)	$I_{D.E.f}$ (μA)	%
-10	**120**	50	0,9	-50	-0,6	**20**	2,01	2,04	+1,5
	120					**60**	2,01	2,12	+5,5
	180					**60**	2,01	2,25	+11,9

Evaluating the results obtained regarding the evolution of $I_{D.E.}$ presented in Table 6.9, it is observed that, the best results were obtained for a duration of 180 s of the production stage and a duration of 60 s for the washing stage.

7. Mass transport studies

Using the values of the limit current (I_L) evaluated by HVL measurements for W.E. from RVC 100 ppi and the calculation formulas from the literature, the mass transport coefficient values (km), and the product km·Av (volume area) and the values for the dimensionless criteria Reynolds for porous electrodes (Rep), Sherwood (Sh), Schmidt (Sc) and Lewis (Le) were calculated and evaluated in comparison with literature data [73-76].

8. Design of a pilot plant for H_2O_2

The technological scheme of a pilot plant for HPE was proposed based on experimental obtained results. This scheme includes FPER, FTHPD and A.W.M..

FPER can be equipped with DSA-O_2 or GB as anode and tested carbonaceous materials (GB, RVC, GF or RGG) as cathode. Depending on the cathode material chosen, the electroactivation protocol can be applied using the auto-adaptive technique proposed in this work.

Material balance calculations were performed to determine the materials requirements to obtain a productivity of 1 kg H_2O_2 /h with a concentration of 1% (1000 ppm) and the voltage balance at FPER level was evaluated during a HPE test using RGG.

9. Purification tests using H_2O_2

The tests for purification of some polluted water samples with methyl blue were made with the Fenton reagent in both homogeneous and heterogeneous phases. For both types of Fenton reagent satisfactory results were obtained but the use of the Fenton reagent in the heterogeneous phase is preferred due to its advantages regarding the efficiency at neutral pH values and the possibility of recovering the solid catalyst at the end of the purification step.

10. General conclusion

The main **personal contributions** are:

A. Elaboration of an experimental stand for HPE study

- The experimental stand includes FPER that allows the HPE study using several types of cathode materials and FTHPD which allows the easy monitoring of the HPE process during the performed tests.

B. HPE tests in potentiostatic mode using 2D and 3D materials

B.1. HPE tests in potentiostatic mode using RVC 100 ppi

In this case, the air was bubbled into the cathode tank and the flow of the electrolyte was directed on the electrode surface parallel to the applied current lines. In these conditions were established:

✓ the starting dates for HPE study through HVL measurements;

✓ the best operating conditions in 1h accumulation tests regarding to electrolyte flow, air flow, applied potential and a long-term accumulation test was made in optimal conditions.

Following the optimization tests it was found that:

- It is necessary to introduce additional air into the system;
- Air bubbling at low flow rates does not ensure efficient oxygenation and air bubbling at is high flow rates leads to a decrease in the efficiency of the HPE which can be caused by the decomposition of H_2O_2 by excessive agitation of the electrolyte solution;
- The starting value for the applied potential established by HVL measurements was confirmed following the tests carried out at its different values.

The unsatisfactory results obtained at the end of the long-term accumulation test (4 h) can be caused by the passivation of the working electrode, the way of introducing the air or the uncontrolled flow of the electrolyte on and through the electrode surface.

B.2. HPE tests in potentiostatic mode using RVC 500 ppi

In this case, the air was bubbled in the catholyte flow and the electrolyte flow was directed through the RVC pores 500 ppi, perpendicular to the applied field lines. Using this type of material were established:

✓ the starting dates for HPE study through VH measurements;

✓ the best operating conditions in 1h accumulation regime regarding the air flow and the potential applied and a long-term accumulation test was made in optimal conditions.

Following the optimization tests it was found that:

• The highest efficiency was obtained at low air flows. By bubbling the air with high flows, large bubbles can be introduced into the REFP which can cause the working electrode surface to become blocked by forming air cushions;

• The tests according to the potential confirmed the correct establishment of the starting value based on the measurements by HVL;

• In the long-term accumulation test (2h) there was also a continuous decrease in the efficiency of the HPE, which can be caused by the air introduction in the system and the difficulty of carrying out a rigorous control of the potential if the air is bubbled in the system.

B.3. HPE tests in potentiostatic mode using GF, GGR and GB

• The process control was impossible because the air bubbles blocked the references electrodes.

In potentiostatic operating mode, the results obtained in terms of H_2O_2 productivity, using RVC 100 ppi and RVC 500 ppi are close (43 ppm respectively 40 ppm), but the results obtained regarding $C.Ef._G$ and $W_{S.G}$ are the best using RVC 100 ppi. Even in this case, the HPE study is continued using the RVC 500 ppi (called RVC) due to the electrolyte flow possibilities it presents.

C. HPE tests in galvanostatic mode using different carbonaceous materials

In this case, the air was bubbled into the catholyte stream and then the two streams were introduced into a centrifugal pump used as an air-electrolyte mixer.

C.1. HPE tests using commercially available carbon materials: GB, RVC and GF

By comparing the results obtained under optimal conditions for each material it was found that:

• The highest productivity was obtained using PG but in this case was obtained the lowest $C.Ef._G$ and the highest $W_{S.G}$;

• Using GB the results are satisfactory in terms of $C.Ef._G$ and $W_{S.G}$ but the productivity is very low;

• The most efficient material among the ones tested in this case is RVC. In this case, a satisfactory productivity is obtained with the best values for $C.Ef._G$ and low values or $W_{S.G}$;

• The satisfactory results obtained at the end of the long-term accumulation test, (after 6 h), using RVC confirm that:

- the new way of introducing air into the FPER is efficient;
- galvanostatic operation is beneficial.

C.2. HPE tests using recycled materials: RGG

• A cathode of graphite granules recovered from spent Zn-C batteries was made;

• The results obtained under optimal conditions using GGR are satisfactory, taking into account the type of material used and the minimum preparation carried out before using them.

D. Comparison of performances using all types of materials tested in galvanostatic operating mode

• The values obtained for C.Ef using GGR are close to those obtained with PG and GB and the values obtained for $W_{S.G}$ are similar to those obtained for using all types of tested materials;

• GGR is a very cheap and promising alternative to commercially available carbonaceous materials (GB, RVC and GF);

• GGR productivity can be increased by applying surface activation techniques. In this context, it was decided to test the possibilities of in situ electroactivation of GGR.

E. In situ electroactivation tests of GGR

E.1. In situ electroactivation tests in 3 stages: production, oxidation and reduction

• Regardless of the values of the electrical parameters applied in the oxidation stage and in the reduction stage, unsatisfactory results regarding to GGR efficiency was achieved.

E.2. In situ electroactivation tests in 4 stages: production, oxidation, reduction and washing

• Under the optimum conditions established for the production and washing stage, the GGR efficiency has been maintained over time, which means that the GGR performance can be improved by applying this type of activation protocol.

F. Design of an installation for HPE

F.1. Proposal of a technological scheme for pilot installation for HPE

• The scheme proposed includes all the equipment necessary for the monitoring and the execution of the HPE and it can be operated under accumulation regime with or without applying the cathode material activation protocol.

F.2. Material balance calculations

• The necessary materials have been established in order to obtain a productivity of 1 kg H_2O_2/h with a concentration of 1%.

F.3. Evaluation of the voltage balance within the FPER during HPE tests

G. Purifications tests using the Fenton reagent

G.1. Purification tests using the homogeneous and heterogonous Fenton reagent

• Complete degradation is achieved in optimal established conditions using both types of reagent.

In order to transpose the purification process on an industrial scale, it is preferred to use the Fenton reagent in heterogeneous phase due to the advantages it presents (high efficiency at neutral pH values, possibility of using a solid catalyst that can be recovered at the end of the purification test).

G.2. An operational scheme for coupling the purification process with the HPE process has been proposed.

The possibility of using GGR for HPE opens new research directions that can be oriented towards increasing HPE efficiency by establishing the optimum thickness of the granule layer and by applying the established activation protocol. Also, the possibilities of coupling the HPE process using GGR with purification processes of different categories of pollutants can be tested.

Selective References

[1] **V. Poza-Nogueiras, E. Rosales, M. Pazos, M. A, Sanroman,** *Chemosphere*, **2018**, 201, 399.

[2] **I. Sires, E. Brillas, M.A. Oturan, M.A. Rodrigo, M. Panizza**, *Environ. Sci. Poll. Res.*, **2014**, 21, 8336.

[3] **P. V. Nidheesh, R. Gandhimathi,** *Desalination*, **2012**, 299, 1.

[4] **M. A. Oturan, M. Zhou, I. Sirés**, *Springer*, **2018,** 61.

[5] **R. L. Myers**, *Greenwood Press, United States of America*, **2007.**

[6] Global Industry Analists, Inc. (GIA): *https://www.strategyr.com/MarketResearch/market-report-infographic-hydrogen-peroxide-forecasts-global-industry-analysts-inc.asp*, Accessed in: September 2019

[7] **E. Brillas, C. A. Martínez-Huitle**, *Appl. Catal. B: Environ*., **2015**, 166-167, 603.

[8] **F. C. Moreira, R. A. R. Boaventura, E. Brillas, V. J. P. Vilar**, *Appl. Catal. B: Environ.*, **2017**, 202, 217.

[9] **S. Garcia-Segura, J. D. Oconb, M. N. Chong**, *Process Saf. Environ. Prot*., **2018,** 113, 48.

[10] **M. A. Oturan, M. Zhou, I. Sirés**, *Springer*, **2018,** 61.

[11] **H. Monteil, Y. Péchaud, N. Oturan, M. A. Oturan**, *Chem, Eng. J*., **2019,** 376, 119577.

[12] **H. Mohammadi, B. Bina, A. Enrahimi**, *Process Saf. Environ. Prot*., **2018**, 117, 200.

[13] **S. O. Ganiyu M. Zhou, C. A. Martínez-Huitle**, *Appl. Catal. B: Environ*., **2018**, 235, 103.

[14] **G. Santana-Martínez, G. Roa-Morales, E. Martin del Campo, R. Romero, B.A. Frontana-Uribe, R. Natividad**, *Electrochim. Acta*, **2016**, 195, 246.

[15] **E. Brillas, I. Sires, M.A. Oturan,** *Chem. Rev.*, **2009**, 109, 6570.

[16] **G. Goor, J. Glenneberg, S. Jacobi**, *Wiley-VCH Verlag GmbH & Co. KGaA,Weinheim*, **2007,** 1.

[17] **B. Šljukić, C.E. Banks, R.G. Compton**, *Journal of the Iranian Chemical Society*, **2005**, 2, 1.

[18] **P. Ilea**, *Editura Casa Cărţii de Ştiinţă, Cluj-Napoca*, **2005.**

[19] **W. P. Mounfield, A. Garg, Y. Shao-Horn, Y. Roman-Leshkov**, *Chemistry*, **2018,** 4, 16.

[20] **E. Petrucci, A. Da Pozzo, L. Di Palma**, *Chem. Eng. J.*, **2016**, 283, 750

[21] **E. Peralta**, *Sustainable Environment Research*, **2013**, 3, 259.

[22] **F. C. Walsh, L. F. Arenas, C. Ponce de León, G. W. Reade, I. Whyte, B. G. Mellor**, *Electrochim. Acta*, **2016**, 215, 566.

[23] **B. Ramírez-Pereda, A. Álvarez-Gallegos, J. G. Rangel-Peraza, Y. A. Bustos-Terrones**, *J. Environ. Manage.*, **2018,** 213, 279.

[24] **J. Li, Z. Ai, L. Zhang**, *J. Hazard. Mater.*, **2009**, 164,18.

[25] **X. Yu, M. Zhou, G. Ren, L. Ma**, *Chem. Eng. J*., **2015**, 263, 92.

[26] **G. Xia, Y. Lu, H. Xu**, *Electrochim. Acta*, **2015**, 158, 390.

[27] **N. Li, S. Wang, J. An, Y. Feng**, *Sci. Total Environ.*, **2018,** 630, 308.

[28] **L.F. Castenada, F. C. Walsh, J. L. Nava, C. Ponce de Leon**, *Electrochim. Acta*, **2017**, 258, 1115.

[29]**J. M. Friedrich, C. Ponce-de-Leon, G. W. Reade, F. C. Walsh**, *J. Electroanal. Chem*., **2004**, 561, 203.

[30] **W. Xing, M. Yin, Q. Lv, Y. Hu, C. Liu, J. Zhang**, Oxygen solubility, diffusion coefficient and solution viscosity, **2014**, Cap. 2,

[31] **Z. Qiang, J.-H. Chang, C.-P. Huang**, *Water Res*., **2002**, 36, 85.

[32] **W. Zhou, L. Rajic, Y. Zhao, J. Gao, Y. Qin,A. N. Alshawabkeh**, *Electrochim. Acta*, **2018,** 277, 185.

[33] **T. Pérez, G. Coria, I. Sirés, J. L. Nava, A. R. Uribe,** *J. Electroanal. Chem.*, **2018**, 812, 54.

[34] **F. Yu, M. Zhou, L. Zhou, R. Peng**, *Environ. Sci. Technol. Lett.*, **2014**, 1, 320.

[35] **F. Yu, M. Zhou, X. Yu**, *Electrochim. Acta*, **2015,** 163, 182.

[36] **E. Rosales, M. Pazos, M.A. Longo, M.A. Sanromán**, *Chem. Eng. J*., **2009**, 155, 62.

[37] **Y. Lu, G. Liu, H. Luo, R. Zhang**, *Electrochim. Acta*, **2017,** 248, 29.

[38] **M. Giomo, A. Buso, P. Fier, G. Sandonà, B. Boye, G. Farnia**, *Electrochim. Acta*, **2008,** 54, 808.

[39] **K. Scott**, *Renewable and Sustainable Energy Reviews*, **2018**, 81, 1406.

[40] **A. Khataee, S. Sajjadi, S.R. Pouran, A. Hasanzadeh, S.W. Joo**, *Electrochim. Acta*, **2017**, 244, 38

[41] **G. Divyapriya, I. Nambi, J. Senthilnathan**, *Chemosphere*, **2018**, 209, 113.

[42] **Y. Wang, Y. Liu, K. Wang, S. Song, P. Tsiakaras, H. Liu**, *Appl.Catal. B: Environ.*, **2015**, 165, 360.

[43] **L. Zhou, Z. Hu, C. Zhang, Z. Bi, T. Jin, M. Zhou**, *Sep. Purif. Technol*., **2013**, 111, 131.

[44] **L. Zhou, M. Zhou, C. Zhang, Y. Jiang, Z. Bi, J. Yang**, *Chem. Eng. J*., **2013,** 233, 185.

[45] **C. Vlaic, S. A. Dorneanu, P. Ilea**, *Studia Universitatis "Babeş-Bolyai", Seria Chimia*, **2009,** LIV Sp. Iss 1, 135.

[46] **C. Vlaic, S. A. Dorneanu, P. Ilea**, *Studia Universitatis "Babeş-Bolyai", Seria Chimia***, 2011**, LVI, June, 2, 167.

[47] **A. Asghar, A. A. A. Raman, W. M. A. W. Daud, M. Ahmad, S. U. B. M. Zain**, *Journal of the Taiwan Institute of Chemical Engineers*, **2017,** 76, 89.

[48] **L. Zhou, M. Zhou, Z. Hu, Z. Bi, K.G. Serrano**, *Electrochim. Acta*, **2014**, 140, 376.

[49] **Z. Pan, K. Wang, Y. Wang, P. Tsiakaras, S. Song**, *Appl. Catal. B: Environ*., **2018**, 237, 392.

[50] **F. Yu, M. Zhou, X. Yu**, *Electrochim. Acta*, **2015**, 163, 182.

[51] **C. A. Martinez-Huitle, M. A. Rodrigo, I. Sires, O. Scialdone**, *Chem. Rev*., **2015**, 115, 13362.

[52] **J. Kim, D. Kwon, K. Kim, M. R. Hoffmann,** *Environ. Sci. Technol*., **2014,** 48, 2059.

[53] **H. Luo, C. Li, X. Sun, B. Ding**, *J. Electroanal. Chem*., **2017**, 792, 110.

[54] **L. Oniciu, L. Mureşan**, *Presa Universitară Clujană*, **1998**, 116.

[55] **S. A. Dorneanu, A. D. Marincean, P. Ilea**, *Studia UBB Chemia*, **2016**, LXI, 155.

[56] **A. D. Mărincean**, **S. A. Dorneanu, P. Ilea**, *Poster at Symposium SICHEM – 2016*, 8-9 September **2016**, Bucharest.

[57] **A. D. Mărincean, S. A. Dorneanu, P. Ilea**, *Poster at RICCCE 20 – 2017*, 6-9 September **2017**, Poiana Braşov.

[58] **A. D. Mărincean, S. A. Dorneanu, P. Ilea**, *Revista de chimie*, **2020,** 8, In press

[59] **T. Ling, B. Huang, M. Zhao, Q. Yan, W. Shen**, *Bioresour. Technol*., **2016,** 203, 89.

[60] **X. Li, I. Angelidaki, Y. Zhang**, *J. Power Sources*, **2017,** 341, 357.

[61] **J. F. Pérez, J. Llanos, C. Sáez, C. López, P. Cañizares, M. A. Rodrigo**, *Electrochim. Acta*, **2017**, 246, 466.

[62] **J. F. Pérez, J. Llanos, C. Sáez, C. López, P. Cañizares, M. A. Rodrigo**, *Sep. Purif. Technol*., **2019**, 208, 123.

[63] **F. Pérez, J. Llanos, C. Sáez, C. López, P. Cañizares, M. A. Rodrigo**, *Electrochem. Commun.*, **2018**, 89, 19.

[64] **J.F. Pérez, J. Llanos, C. Sáez, C. López, P. Cañizares, M.A. Rodrigo**, **2016,** 71, 65.

[65] **C. T. Wang, J. L. Hu,W. L. Chou, Y. M. Kuo**, *J. Hazard. Mater*., **2008**, 152, 601.

[66] **H. Zhang, Y. Li, H. Zhang, G. Li, F. Zhang**, *Sci. Rep*., **2019**, 9:1817, 1.

[67] **N. W. Tata**, **S.A. Dorneanu**, **A. D. Mărincean,** *Master Thesise, Cluj-Napoca*, **2019.**

[68] **A. D. Mărincean, S. A. Dorneanu, P. Ilea**, *Poster at Symposium SICHEM – 2018*, 6-7 September **2018**, Bucharest.

[69] **Barbara de Oliveira, R. Bertazzoli**, *J. Electroanal. Chem*., **2007**, 611, 126.

[70] **A. Chmayssem, S. Taha, D. Hauchard**, *Electrochim. Acta*, **2017**, 225, 435.

[71] **C.A. Vlaic, S.A. Dorneanu**, *Studia UBB - Chemia*, **2015**, LX(3), 141.

[72] **W. Zhou, J. Gao, K. Kou, X. Meng, Y. Wang, Y. Ding, Y. Xu, H. Zhao, S. Wu, Y. Qin**, *Journal of the Taiwan Institute of Chemical Engineers*, **2018,** 83, 59.

[73] **P. H. F.J. Recio, L. Vazquez, C. Ponce de León, F.C. Walsh**, *Electrochim. Acta*, **2013,** 90, 507.

[74] **F. F. Rivera, C. P. de León, J. L. Nava, F. C. Walsh**, *Electrochim. Acta*, **2015,** 163, 338.

[75] **A.H. Sulaymon, A.H. Abbar**, *Electolysis*, **2012**, Cap. 9, 190.

[76] **V. Reyes-Cruza, I. González, M.T. Oropez**, *Electrochim. Acta*, **2004**, 49, 4417.